Proceedings of the 17th World Congress
The International Federation of Automatic Control
Seoul, Korea, July 6-11, 2008

Analysis of the Oil Film Effect in the Air Gap of an Electro-hydraulic Compound Pump

Sheng-Ping Hsieh*. Thong-Shing Hwang.**
Min-Tzung Hwang***

** Graduate Institute of Electrical and Communication Engineering, Feng Chia University, Taichung, Taiwan 407, R.O.C. (e-mail: hsp48.johnson@msa.hinet.net).*
***Department of Automatic Control Engineering, Feng Chia University, Taichung, Taiwan 407, R.O.C. (e-mail: tshwang@fcu.edu.tw)*
**** Chung-Shan Institute of Science and Technology, Taichung, 40722 Taiwan, R.O.C. (e-mail: arvin@wctv.tinp.net.tw)*

Abstract: The electro-hydraulic compound pump is a new integrated product, in which the pump and motor are combined as one unit replacing the traditional connection with a shaft coupling. A piston pump embedded in the motor rotor is capable of actuating the pump without a rotating shaft coupling. There are a great deal of advantages in this design, such as reduced noise, decreased power loss, and easy installation. The piston pump body is placed in the motor rotor because of the compound pump design. The air gap between the rotor and motor stator is filled with hydraulic oil. The rotor is directly rotated in the hydraulic oil. The control of the pressure and flow is achieved by means of the mechanical adjustment at the pressure valve. This paper adopts the Maxwell EM software matched with the corresponding mathematical theory to examine and simulate the oil film effect in the air gap on the electrical performance of an electro-hydraulic compound pump. The experimental results are given.

1. INTRODUCTION

A fluid, usually oil, is the lifeblood of a machine and does the job of distributing and transferring energy from the prime mover (typically an internal combustion engine or electric motor) through control valves to the load, for example, actuators like cylinders or motors. The electro-hydraulic compound pump is an integrated product that is a functional piston pump and motor combination. The pump case is inserted as a part of the motor rotor. The advantages are 10-15% noise reduction, 30% energy savings and 10% reduced cost. For industrial applications, the compound pump can be fabricated using standard industrial technological advances, including design, analysis, manufacturing, assembly and testing. These technical levels indicate that the compound pump operations require high pressure, large flow, and precise positioning. New compound pump features allow for modern control methods that can lead to higher efficiencies. These are practically identical to those of any industry or engineering project.

Recently Yannis et al. (2006) proposed an active electro-hydraulic pump system analysis. A great deal of effort has been made by Dynex, Eaton, and Daikin industries LTD. What seems to be lacking, however, is a performance analysis. Electro-hydraulic compound pumps like this one are designed with closed-loop, servo-controlled displacement components. This paper studies the electrical performances for an electro-hydraulic compound pump, including the oil film effects in the air gap between the stator and rotor. The influence of the three groups of variables: oil film coefficient of viscosity, oil temperature, and air gap are examined. According to the test procedure specifications (Hwang, 2006), there are many types of testing approaches for pumps, such as the water pressure test, pressure proof test, endurance test, functional test, worn-in test, and so on. We will concentrate on the functional test.

The purpose of this analysis is to develop a compound pump that has high efficiency and can overcome the heating problem. This analysis is primarily concerned with the oil film influence in the air gap to ensure optimal air gap design via the simulation analysis to verify the experimental formula (Liu, 2004). The rest of this article is organized as follows: Section 2 describes the electro-hydraulic compound pump and lists the preliminary design specifications and relevant parameters. Section 3 gives a brief plan of the concept of the electro-hydraulic pump control system. The modified control signal suited to the pump being considered is proposed. Section 4 describes the oil film effect. We start with the mathematical formula, followed by simulations using the package software：Maxwell EM and Hypneu. For details please refer to the Appendix. A comparison of hydraulic fluid with oil temperature and the viscosity coefficient is also presented. Section 5 provides the experimental results and simulation performance. Experimental operations are used to validate the proposed design technique. Section 6 discusses the oil film effect, which can be classified into three main portions. Our conclusions and future work based on the relative analyses are given in Section 7.

2. ELECTRO-HYDRAULIC COMPOUND PUMP

The structure of the electro-hydraulic compound pump is a rotor combined with a piston pump, as shown in Figure 1. The rotor is combined with the stator on an outer frame to make a motor-pump set without the need for a coupler. Figure 2 below shows the electro-hydraulic pump.

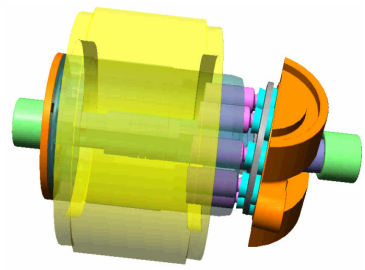

Fig. 1. Rotor for compound piston pump

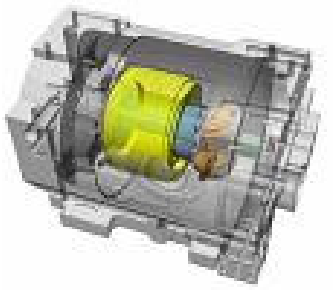

Fig. 2. 3D diagram of an electro-hydraulic compound pump with the stator and rotor

In this design concept, we set a preliminary specification and refer to the design handbook (Hamdi, 1994; Liu and Hsu, 1986) to obtain a series of corresponding parameters, as shown in Table 1.

Table 1. The Preliminary specifications and relevant parameters for an electro-hydraulic pump

Input voltage	AC 220V
Frequency	60Hz
Rated current	5.8A
Rated rotating	1710 rpm
Power factor	0.8
Output power	1.5 kw
Phase, pole	3Φ, 4P
Efficiency	0.85
Rated load*	8.13 N m
Max. load*	24.39 N m
Stator slot	48 slots
Rotor slot	60 slots
Stator turn per slot	48 turns
Wire diameter of stator	0.65 mm
Wiring connection of stator	2Y, concentric winding
Pitch factor (kp)”	0.966
Distribution factor (kd)”	0.958
Winding factor (kw)”	0.925

* Experience formula were given from reference data
” The data were collected from the check table

This design was produced using the above specifications. The design handbook process was used to design the electro-hydraulic pump. We also referenced the configurations of related foreign products. The design parameters were obtained and input into the Maxwell EM software to set up the electro-hydraulic pump model. The simulation analyzed the static and dynamic fields. After affirming the related design size, material, and shape, the electro-hydraulic compound pump met the preliminary prototype design. However, we found very little relevant data in the motor design literature. In particular, it is very rare that a rotor and stator are both immersed in hydraulic oil without the motor design data. The data for hydraulic oil electrical performance was difficult to obtain. Therefore, we began this study on the influence and effect of hydraulic oil in the air gap between the stator and rotor. These results will be used to establish a basic electro-hydraulic compound pump design.

3. SCHEME OF CONTROL SYSTEM

At present, the control of the pressure and flow in the electro-hydraulic compound pump is achieved by means of the setting of the output pressure at a mechanical pressure valve, and then an output flow that depends on the angle of tilting disk is generated at the control valve. Therefore, future research is obviously required, but this is an exciting first step. We will add to some components in the compound pump, including the following: pressure sensor, flow sensor, inverter, and single chip microcomputer. The framework with an electrical signal way is given for controlling output pressure and flow of the electro-hydraulic compound pump. The electrical signal is provided to the proportional solenoid. The output pressure and flow of the compound pump is controlled based on the electrical signal to the proportional solenoid. The operation of the closed loop control system corresponding to these flow and pressure is illustrated in the block diagram of Figure 3.

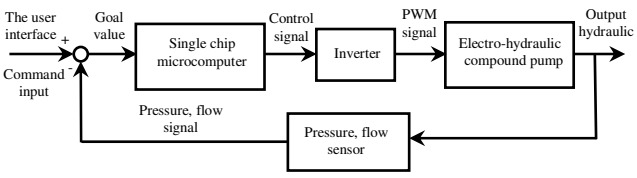

Fig. 3. Block diagram of the control system for electro-hydraulic pump

As the above diagram indicates, the output fluid of the electro-hydraulic compound pump is controlled based on the electrical signal. With this scheme, response velocity of the pressure and flow become faster than that of the traditional mechanical approach; besides, the environmental protection goal of energy saving of frequency conversion can be accomplished.

4. EFFECT OF OIL FILM

The oil film effect arises from the hydraulic oil in the air gap between rotor and stator. This is expressed in form (1) (Fitch and Hong, 1997).

$$T = 4\pi^2 r^3 \mu \omega_m \frac{\omega}{h} \tag{1}$$

Where T is the torque, r is the rotor radius, μ is the coefficient of viscosity, ω_m is the rotational speed, ω is the stator and rotor stack thickness, and h is the size of the air gap.

Form (1) clearly shows that there are five major variables that affect the oil film viscosity force. Commercial products do not easily achieve changes in rework or improved performance due to lack of techniques. Therefore, let us begin with a realizable industry process in which the air gap size and coefficient of viscosity for hydraulic oil are the parameters in a relatively easy process. The issues are discussed from the influence of the oil film effect on the electro-hydraulic compound pump yielded by every parameter between the coefficient of viscosity for different oils and air gaps. In the beginning, we choose two types of military specification hydraulic fluids (Mil-H-5606B, Mil-H-83282) used often in the aviation industries for comparative analysis. The relevant parameters are shown in Table 2.

Table 2. The comparison between the coefficient of viscosity for hydraulic fluids at different temperatures

Temperature (degrees C)	Hydraulic fluid (Cst)	
	Mil-H-5606B	Mil-H-83282
-53.9	2130.0	9554.0
-40.0	500.0	5132.0
-28.9	Non	642.1
-17.0	100.0	193.4
37.0	14.3	Non
98.0	2.1	Non

Non is expressed as “without relevant data in Hypneu software”

The coefficient of viscosities for the hydraulic fluids listed in Table 2 were obtained from the Hypneu simulation software. The working environments for these hydraulic fluids are so different that the corresponding oils also have different coefficients of viscosity. From Table 2, we find that the hydraulic oils with different attributes exhibit changes in the coefficient of viscosity at the same working temperature range.

In addition, as the different oil products represent different coefficients of viscosity and the pump operating temperature is fixed at a temperature range under normal conditions, one can settle the oil temperature and the coefficient of viscosity range by employing hydraulic fluids with different temperatures to match the desired coefficient of viscosity. To do this we focus on the influence of three groups of variables: oil film coefficient of viscosity, oil temperature and air gap. This study simulates and discusses the parameter properties for three types of temperatures -17 degrees C, 37 degrees C, and 98 degrees C in the Mil-H-5606B.

5. SIMULATION ANALYSIS AND TEST EXPERIMENT

5.1 Simulation analysis

The design size was obtained via simulation analysis. The output property towards the actual output was affirmed afterwards. One then begins to progress at transient simulation analysis on the change in oil film, temperature and air gap. To start with, we employed the present air gap design specifications at 0.35mm thickness. Making the simulation under such oil film free conditions, and the results appear in Figure 4. From the velocity and torque model output response curve one can observe the basic electrical performances in the no-load and without oil film case.

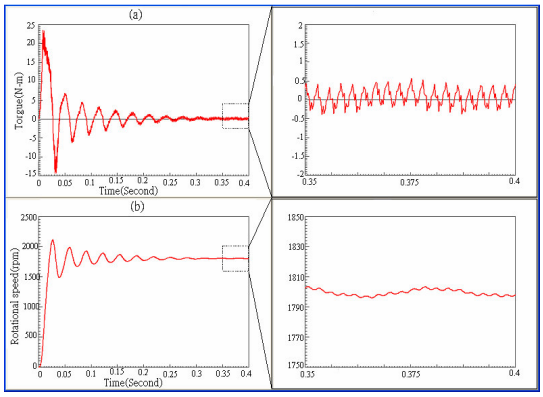

Fig. 4. (a) Torque output curve at 0.35mm air gap and oil film free (b) Rotational speed output curve under the same conditions

Added to the oil film effect simulation analysis, we joined the oil film property of Mil-H-5606B hydraulic oil with three temperatures, -17 degrees C, 37 degrees C, and 98 degrees C, respectively. After simulation analysis, the transient output results were obtained as shown in Figures 5, 6 and 7.

Additionally, we changed the air gap size from 0.35mm to 0.2mm for the electro-hydraulic compound pump and employed the Mil-H-5606B hydraulic oil film characteristics at 37 degrees C to perform the transient simulation analysis. The simulation results are shown in Fig. 8. We arranged the viscosity torque yielded using the oil film in Figures 5-8 into

Fig. 9 to clearly distinguish and examine the three groups of variables: oil film coefficient of viscosity, oil temperature and air gap.

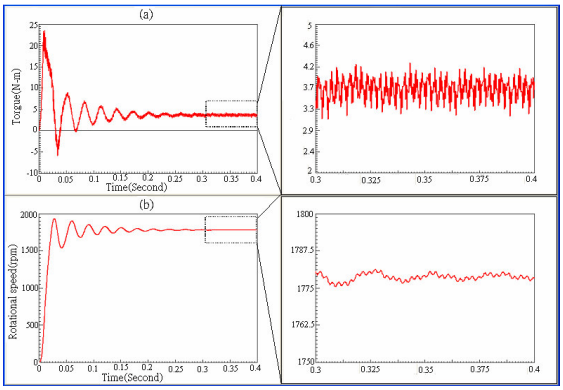

Fig. 5. (a) Torque output curve at 0.35mm air gap and -17.0 ℃ oil film (b) Rotational speed output curve under the same conditions

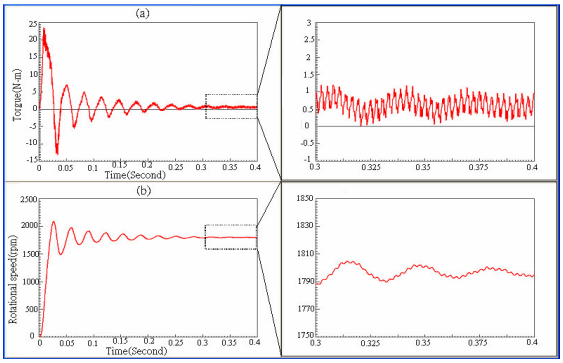

Fig. 6. (a) Torque output curve at 0.35mm air gap and 37℃ oil film (b) Rotational speed output curve under the same conditions

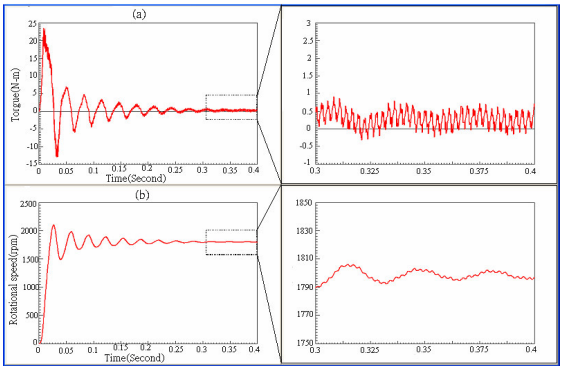

Fig. 7. (a) Torque output curve at 0.35mm air gap and 98℃ oil film (b) Rotational speed output curve under the same conditions

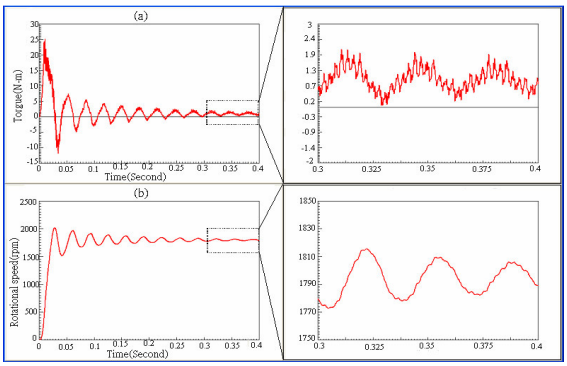

Fig. 8. (a) Torque output curve at 0.2mm air gap and 37℃ oil film (b) Rotational speed output curve under the same conditions

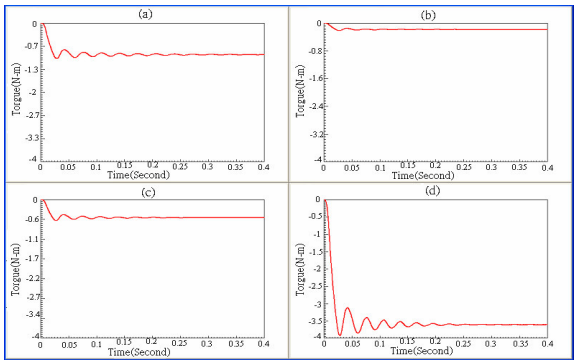

Fig. 9. Viscosity torque output (a) under the 0.2mm air gap and the oil film temperature of 37℃ (b) at 0.35mm air gap and 98℃ oil film (c) at 0.35mm air gap and 37℃ oil film (d) at 0.35mm air gap and -17.0℃ oil film

5.2 Test experiment

The electro-hydraulic compound pump involves an electric motor and pump integrated into the same outer frame. This pump specification has never had defined test methods. Accordingly, the test procedure for the electro-hydraulic pump contains a reference to the test specification for a general piston/impeller pump (ASTM, 2003; SAE,1996) and three-phase induction motor (CNS,1999). To take an example from the EHP15-15 type electro-hydraulic pump (see Fig. 10), the test methods and results will be briefly described in the following paragraph.

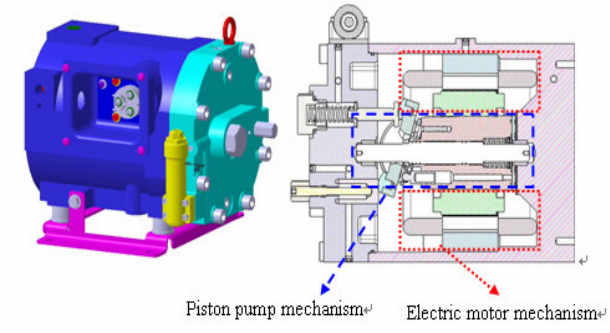

Fig. 10. Schematic diagram of type EHP15-15

After the worn-in test, qualified products may proceed to the function test referring to the test procedure for an electro-hydraulic compound pump(Wu, 2006). The test items include:

- Flow adjustment range test;

- Noise test;

- Leakage test; and

- Pressure-flow characteristic test.

As the first step in our test, we placed the electro-hydraulic pump onto a stand for testing the working tank and connected an inlet port, outlet port, and drain pipe with a thermocouple and tachometer installed in the appropriate measurement locations. The sensors confirmed that they do not fall from their position. The remaining functional tests were performed step by step. Experiments were performed to prove the development for the electro-hydraulic pump of type EHP15-15, the solid test appears in Figure 11. An entire flow road for the test stand is shown in Figure 12. Table 3 summarizes the pressure-flow characteristic test results among the test items.

Fig. 11. Solid test for an electron-hydraulic pump of type EHP15-15

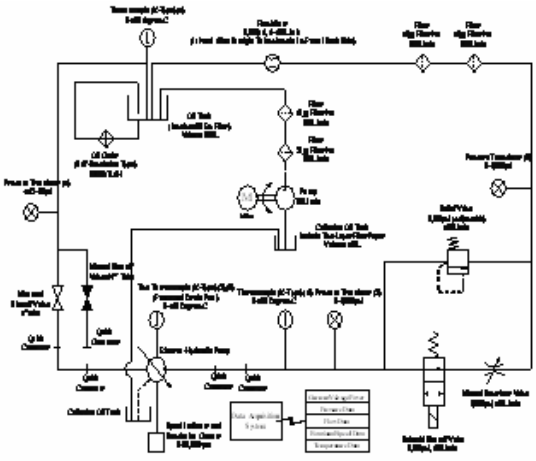

Fig . 12. Flow road of the test stand

Table 3. Relevant data of pressure-flow characteristics test*

Test condition		Voltage (V)	Pressure (kg/cm^2)			Temperature (℃)			
			①	②	③	①	②	③	④
Current 5.8A (100%)	Max. flow 30 L/min	223.6	0	31.2	3.4	35	44	45	38
	25 L/min	223.1	0	35.8	3.3	35	45	49	39
	20 L/min	223.1	0	43.3	3.3	35	46	50	39
	15 L/min	220.1	0	49.8	3.3	35	46	51	39
	10 L/min	220.1	0	60.2	3.3	35	47	52	39
	5 L/min	223.0	0	74.6	3.3	36	48	52	39
	3 L/min	223.1	0	89.4	3.3	36	49	52	40
Current 8.7A(150%)	Max. flow 30 L/min	221.6	0	60.5	3.4	35	47	49	37
	25 L/min	220.0	0	66.8	3.4	35	48	52	38
	20 L/min	222.0	0	75.7	3.3	35	48	53	38
	15 L/min	222.0	0	91.1	3.3	35	49	54	39
	10 L/min	222.5	0	105.8	3.3	35	50	54	39
	6.8 L/min	219.8	0	112.9	3.3	35	48	51	40
Current 11.6A(200%)	Max. flow 30 L/min	221.0	0	83.7	3.3	35	48	48	38
	25 L/min	221.6	0	89.6	3.3	35	48	52	38
	20 L/min	221.6	0	97.3	3.3	34	48	53	38
	15 L/min	221.9	0	113.6	3.3	35	49	53	39
	10 L/min	221.4	0	135.3	3.3	34	50	54	39
	6.6 L/min	221.1	0	152.9	3.3	34	50	54	39

* The data were obtained under the rotational speed as zero

Note: Labels ①,②,③, and ④ are the sensors' number, locations appear in Fig. 12.

After obtaining the accurate performance data, the results are as follows:

- Drawing out pressure-flow characteristic curve from Table 3, as shown in Figure 13, it was found from the characteristic curve that the pressure was inversely proportional to the flow. The larger the pressure, the smaller the flow. The current at 8.7 amperes was in the optimal range.

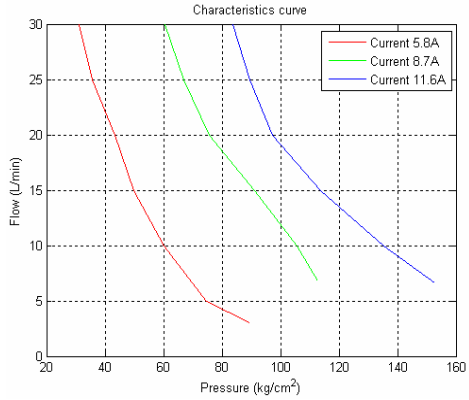

Fig. 13. Pressure-flow characteristic curve

- Maximum flow (Q) in the pump is 26.5L/min, leakage flow (Qdrain) equals 0.3L/min. While the pump flow is 0L/min, the pressure adjustment is up to 3000psi, from which the pump can be represented as bearing the pressure at 3000psi.

Table 4. The oil film effect in air gap at a 0.35mm thickness

Item / Oil film temperature	Coefficient of viscosity (Unit:Cst)	No-load starting torque	Oil film load output *	No-load steady-state rotation(*rpm*)
-17.0℃	100.0	23.5 $N \cdot m$	3.610 $N \cdot m$	1780
37℃	14.3	23.55 $N \cdot m$	0.520 $N \cdot m$	1797
98℃	2.1	23.5 $N \cdot m$	0.185 $N \cdot m$	1798
Oil film free	0	23.5 $N \cdot m$	0 $N \cdot m$	1799

* Output condition was "under the steady-state rotation"

From the analysis in Table 4, the oil film output characteristic under no-load conditions has the load effect, and the load size is determined by the coefficient of viscosity of the hydraulic oil. When the coefficient of viscosity is large, the torque load yielded by the oil film air gap for the electro-hydraulic will grow larger. Further, the load output is proportional to the variation for a large coefficient of viscosity. For example, the coefficient of viscosity for the oil film at -17.0 degrees C becomes 6.99 times as much as that at 37 degrees C. The viscosity of the oil film at -17.0 degrees C produced 6.94 times as much load effect at 37 degrees C. This value can be explained by form (1). What causes of the difference between the multiple load effect in oil film viscosity and the multiple coefficients of viscosity at -17.0 degrees C and 37 degrees C? There are two reasons for this judgment: 1. the load stems from the coefficient of viscosity which affects the rotational output and the rotational frequency is a significant parameter in the load yielded by the coefficient of viscosity. 2. The load value also leads to its relative reduction. The influence of the rotor inertia and friction coefficient on bearing is another reason. Although the inertia and friction force are not large for the compound pump, an oil film with a small coefficient of viscosity has greater influence.

6.2 The influence of oil temperature or different hydraulic oil

One can find from Table 2 that different oil temperature results in a different coefficient of viscosity for hydraulic fluid. Observing from Figures 5-7 that the torque characteristic output curve has a different torque output under no-load rated speed conditions. This is the load torque yielded by the hydraulic oil also has a relative difference under the different temperatures; i.e., -17.0 degrees C, 37 degrees C, and 98 degrees C. The change in the coefficient of viscosity is the reason. Different hydraulic oils also have different coefficients of viscosity. Therefore, the different coefficient of viscosity induces different hydraulic oil temperatures equivalent to that in the different types of hydraulic oils. Therefore, the different oil temperatures and different hydraulic oils commonly affect the change in coefficient of viscosity. Its influences can be interpreted in (1) as a linear proportional change under ideal conditions: constant speed, without loss, and without friction. The coefficient of viscosity of hydraulic oil at 100Cst produces 10 times as much viscosity force as that of hydraulic oil at 10Cst.

6.3 The influence of air gap change

We use Figures 6, 8, and 9 for comparison and analysis on the influence of the change in air gap between the rotor and stator. The dynamical analysis on the air gap thickness used two types of specifications: 0.25mm and 0.35mm. The data are arranged in order from the characteristic curve, as shown in Table 5. The change in the air gap makes the variation in torque output on electric starting and viscosity force load from the oil film for the compound pump. Therefore, we analyze the change in starting torque and viscosity oil film load force between air gap thicknesses from 0.2mm to 0.35mm. The changes in air gap were obtained from these three groups of regions; the change from 0.2mm to 0.25mm; second, the change from 0.25mm to 0.3mm; third, the change from 0.3mm to 0.35mm. The starting torque reduces to 1.2%, 2.02%, and 3.72%, respectively. Moreover, the oil film viscosity force load reduces to 0.2%, 0.16 %, and 0.15%, respectively. Therefore, it seems reasonable to support that an air gap designed with 0.3mm is best for these specifications. The moment the air gap becomes too large, the amplitude in change in starting torque grows larger. The amplitude of change in viscosity force kept at the same size and the steady-state rotation does not change under no-load conditions. Thus, an air gap of 0.3mm increases in thickness again, and will reduce the effect**.** While the air gap thickness grows smaller, there are transformations in both the starting torque and viscosity force amplitude. The steady-state rotation also responds with a reduction under no-load conditions. Hence, the air gap of 0.3mm decreases in thickness again and the whole effect is a slight reduction. While the design specifications for the air gap with a thickness of 0.3mm, the difficult points in processing become lower than those of the air gap at a thickness of 0.25mm. Therefore, we propose an air gap with 0.3mm thickness.

Table 5. The change in air gap for compound pump under filling the Mil-H-5606B fluid at 37 degrees C

Item / Air gap size	No-load starting torque	Oil film load output	No-load steady-state rotation (*rpm*)
0.20 *mm*	25.0 *N-m*	0.91 N-m	1793
0.25 *mm*	24.7 N-m	0.73 N-m	1795
0.30 *mm*	24.2 N-m	0.61 N-m	1797
0.35 *mm*	23.3 N-m	0.52 N-m	1797

7. CONCLUSIONS AND FUTURE WORK

From the above, we state the following three points;

1) The oil film in the air gap between the stator and rotor for an electro-hydraulic compound pump yields the load effect and produces extra losses in the electro-hydraulic pump output.

2) The oil film with a lower coefficient of viscosity has a smaller influence with the load effect yielded in the oil film

and reduction in losses. However, hydraulic oil with a low coefficient of viscosity will also reduce pump output efficiency. These points can be clearly observed from Table 3, and the type and temperature for the hydraulic oil can also determine the change in oil coefficient of viscosity. One would therefore estimate the working environment for the electro-hydraulic pump in order to produce the maximum efficiency before using hydraulic oil.

3) The air gap size is a compromise variable. We see from Table 5 that a large air gap can reduce the torque yielded by the oil film, but it will reduce to the electrical efficiency for electro-hydraulic compound pump at the same time. On the other hand, a small air gap can increase the torque. Therefore, determining the design air gap thickness must be in coordination with a working environment, temperature and hydraulic oil coefficient of viscosity. The maximum efficiency can then be obtained from the simulation analysis. Using these analyses for the electro-hydraulic pump and hydraulic oil in this article, we confirmed that an air gap design with a 0.3mm thickness is the optimal specification.

To summarize the preceding analyses and experiment results, one might see that the function of the electro-hydraulic pump correspond to the design specifications and requirements. Based on the test criterion and relative experiments for an electro-hydraulic pump, it can be concluded that the analysis was supported by the experimental results.

Future work will hopefully progress in this important control concern. The performance of the overall control system can be studied suitably from all points of view: the system reacts rapidly to changes in the operation conditions and effectively excludes heat in the fluid occurring on the compound pump; the adjustment achieved supplies very small steady-state errors both for pressure and flow.

ACKNOWLEDGEMENTS

This research was supported by The Ministry of Economic Affairs and National Science Council, Taiwan, R.O.C. under grant # 95-EC-2A-17-0443 and NSC 96-2221-E-035-084.

REFERENCES

American Society for Testing Material Standards (2003). *Standard Guide for Performance Evaluation of Hydraulic Fluids for Piston Pumps*, ASTM D6813. ASTM International, West Conshohocken, PA, USA.

Chinese National Standards (1999a). *Low Voltage Three-phase Induction Motors*, CNS 1056. Bureau of Standards, Metrology and Inspection, M. O. E. A., Taiwan, R.O.C.

Chinese National Standards (1999b). *Calculating Methods of Three-phase Induction Motor Characteristics*, CNS 5421. Bureau of Standards, Metrology and Inspection, M. O. E. A., Taiwan, R.O.C.

Fitch, E.C., and Hong, I.T. (1997). *Hydraulic Component Design and Selection*, page 115. Bardyne Inc. Press, Stillwater, Okla.

Hamdi, E.S. (1994). *Design of Small Electrical Machines,* John Wiley & Sons Press, New York.

Hwang, M.T. (2006). *An Electro-hydraulic Compound Pump Test Report*, Technical Report, CSIST-0443-T303(95). Subsystem Group, Aeronautical Research Lab., Taiwan, R.O.C.

Liu, C.C., and Hsu, Y.Y. (1986). *Electrical Machines--Part Ⅰ*,Third Edition. Central Book Publishing Co. Press, Taipei City, Taiwan.

Liu, H.H. (2004). *Ministry of Economic Affairs Executes Detailed Plans for Technological Projects in 2004*, Project Plan, Aeronautical Research Lab., CSIST, Taiwan, R.O.C.

Society of Automotive Engineers (1996). *Hydraulic Power Pump Test Procedure*, SAE J745. SAE International, USA.

Wu, Y.C. (2006). *An Electro-hydraulic Compound Pump Test Procedure*, Tech. Rep., CSIST-0443-T302(95), Aeronautical Research Lab., Chung-Shan Institute of Science and Technology , Taiwan, R.O.C.

Yannis, K., Anthony, T., and Demosthenes, T. (2006). Multi-Parametric Optimization of a Pulse Width/Phase Modulated Controller a High Frequency Active Electro-Hydraulic Pump System. *Proceedings of the 45th IEEE Conference on Decision & Control*, San Diego, CA, USA, pp. 5335-5340.

APPENDIX

In this study, the brief introductions to the use of software are given below.

• Hypney

The main function of this software is to simulate the dynamic characteristics of a hydraulic system. It is comprised of hydraulic oils and the relevant characteristic parameters. Using the sketch connection operations and after the characteristic parameter setting, one proceeds with this simulation analysis to understand the system performance behaviour. In this paper, the software was used for hydraulic oil characteristic parameter identification without relevant analysis and operation.

• Maxwell EM

The main function of this software is to analyze the magnetic field. The first issue that we will describe is the static aspect; it can analyze magnetic force distribution (see Fig. 14), the size of magnetic force (see Fig. 15), and magnetic line tendency (see Fig. 16); from this analysis action, one may understand that the components are in case of applying a maximum load instantaneous. Its related performance whether meets the requirements; from this result, is it proper to consider the related material or design?

The second issue that we will describe is the dynamic aspect; after the relevant parameters have settled, one can analyze the dynamic performance of the components with related input and output, and the results are shown in this article (see Figures 4-9); one may recognize from these results that the outcomes of static analysis are correct. The components of related magnetic force are sure that the static and dynamic

characteristics meet the requirements to save actual manufacturing failure costs and achieve the beneficial CAD (computer aided design) results. The process of dynamic analysis can directly simulate the output action of the components on types and properties under applying the actual input conditions. For example, in the induction motor part of the study, the output action will exhibit a rotating motion manner and the magnetic line distribution characteristics during motor rotation. One instantaneous dynamic simulation scene is shown in Fig.17.

An introduction to the operation interface, from which all of operation aspect for Maxwell EM is shown in Fig. 18. Through the left-hand side options, one can choose several types of analysis modes: dynamic, static, and eddy current. After this, completing step by step the sketch drawing and the performance parameters setting based on the options, and then deciding on a selection of analysis condition, if so one can accomplish the relative analysis under corresponding to setting regulations. So the software in this paper, it has a large of help for design of induction motor and the rest in such type of the magnetic force components.

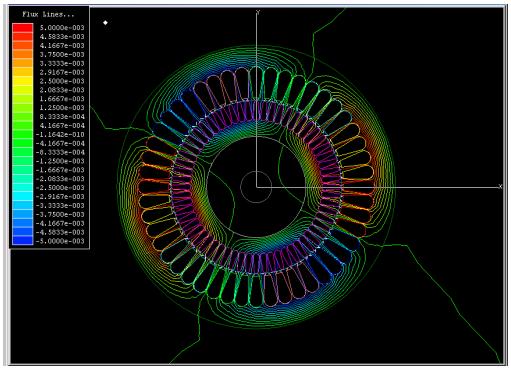

Fig. 14. A distribution diagram of static magnetic force for induction motor in Maxwell EM

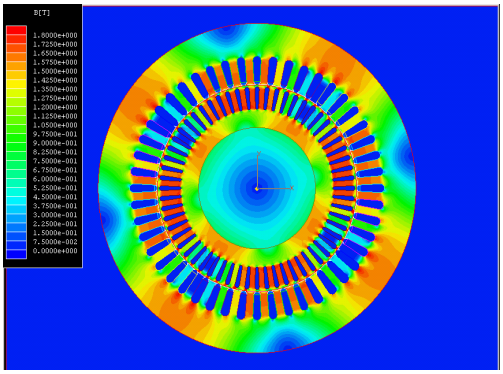

Fig. 15. A size diagram of static magnetic force for induction motor in Maxwell EM

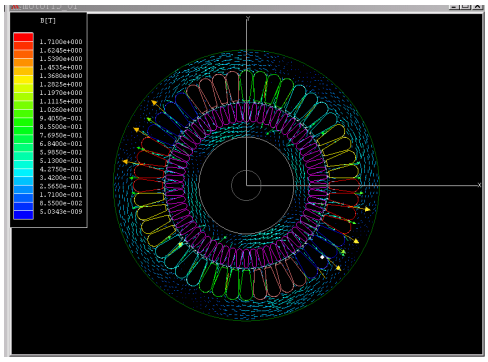

Fig. 16. A tendency diagram of static magnetic force for induction motor in Maxwell EM

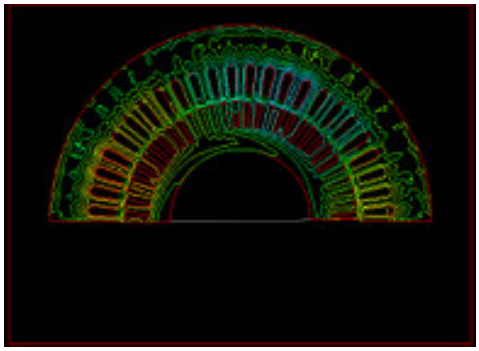

Fig. 17. A simulation scene of dynamic analysis in Maxwell EM

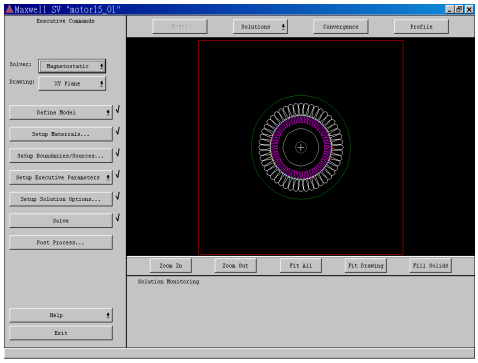

Fig. 18. An analysis operation scene in Maxwell EM